Research Article

NMR IN BIOMEDICINE

Received: 21 May 2009, Revised: 25 June 2009, Accepted: 6 July 2009, Published online in Wiley InterScience: 30 September 2009

(www.interscience.wiley.com) DOI:10.1002/nbm.1432

# Non-invasive detection of glycine as a biomarker of malignancy in childhood brain tumours using *in-vivo* $^1$H MRS at 1.5 Tesla confirmed by *ex-vivo* high-resolution magic-angle spinning NMR

N. P. Davies[a,b,c]*, M. Wilson[a,c], K. Natarajan[a,b,c], Y. Sun[a,c], L. MacPherson[c], M-A. Brundler[c], T. N. Arvanitis[c,d], R. G. Grundy[e] and A. C. Peet[a,c]

**Management of brain tumours in children would benefit from improved non-invasive diagnosis, characterisation and prognostic biomarkers. Metabolite profiles derived from *in-vivo* MRS have been shown to provide such information. Studies indicate that using optimum a priori information on metabolite contents in the construction of linear combination (LC) models of MR spectra leads to improved metabolite profile estimation. Glycine (Gly) is usually neglected in such models due to strong overlap with myo-inositol (mI) and a low concentration in normal brain. However, biological studies indicate that Gly is abundant in high-grade brain tumours. This study aimed to investigate the quantitation of Gly in paediatric brain tumours using MRS analysed by LCModel™, and its potential as a non-invasive biomarker of malignancy. Single-voxel MRS was performed using PRESS (TR 1500 ms, TE 30 ms/135 ms) on a 1.5 T scanner. Forty-seven cases (18 high grade (HG), 17 low grade (LG), 12 ungraded) were retrospectively selected if both short-TE and long-TE MRS ($n = 33$) or short-TE MRS and high-resolution magic-angle spinning (HRMAS) of matched surgical samples ($n = 15$) were available. The inclusion of Gly in LCModel™ analyses led to significantly reduced fit residues for both short-TE and long-TE MRS ($p < 0.05$). The Gly concentrations estimated from short-TE MRS were significantly correlated with the long-TE values ($R = 0.91$, $p < 0.001$). The Gly concentration estimated by LCModel™ was significantly higher in HG versus LG tumours for both short-TE ($p <$ 1e-6) and long-TE ($p = 0.003$) MRS. This was consistent with the HRMAS results, which showed a significantly higher normalised Gly concentration in HG tumours ($p < 0.05$) and a significant correlation with the normalised Gly concentration measured from short-TE *in-vivo* MRS ($p < 0.05$). This study suggests that glycine can be reliably detected in paediatric brain tumours using *in-vivo* MRS on standard clinical scanners and that it is a promising biomarker of tumour aggressiveness.** 

**Keywords:** Magnetic resonance spectroscopy; brain tumours; glycine; children; LCModel; high-resolution magic angle spinning NMR

## INTRODUCTION

Brain tumours account for approximately 25% of childhood cancer and are the most common solid tumours in children. Accurate non-invasive characterisation of childhood brain tumours is important given the diversity of brain tumour types occurring in children and the impact of tumour type, site and age of the patient on their clinical management. Magnetic resonance spectroscopy (MRS) has a significant role to play as it provides the opportunity to study the metabolism of brain tumours non-invasively. Classification of brain tumours using MRS has been shown to permit accurate non-invasive diagnosis of brain tumours (1–3). Recent studies have shown that multivariate analysis of metabolite profiles derived from MRS allows accurate identification and characterisation of adult (4) and childhood (5) brain tumours while providing useful insight into tumour biology. Furthermore, quantitation of individual metabolites can provide important biomarkers of tumour behaviour (6,7).

The use of tools such as LCModel™ (8) to estimate metabolite profiles from MRS data by fitting to a linear combination of model spectra from known metabolites has proved beneficial in such studies (4–6). However, one limitation of these methods is that they depend on the accuracy and completeness of *a priori* knowledge of tissue metabolite contents. Incomplete or

* *Correspondence to: N. P. Davies, Institute of Child Health, Whittall Street, Birmingham, B4 6NH, UK.*
*E-mail: nigel.davies@bch.nhs.uk*

a *N. P. Davies, M. Wilson, K. Natarajan, Y. Sun, A. C. Peet*
*Cancer Sciences, University of Birmingham, Birmingham, UK*

b *N. P. Davies, K. Natarajan*
*Imaging & Medical Physics, University Hospital Birmingham NHS Foundation Trust, Birmingham, UK*

c *N. P. Davies, M. Wilson, K. Natarajan, Y. Sun, L. MacPherson, M. Brundler, T. N. Arvanitis, A. C. Peet*
*Birmingham Children's Hospital NHS Foundation Trust, Birmingham, UK*

d *T. N. Arvanitis*
*School of Electronic, Electrical & Computer Engineering, University of Birmingham, Birmingham, UK*

e *R. G. Grundy*
*Children's Brain Tumour Research Centre, University of Nottingham, Nottingham, UK*

**Abbreviations used:** *CPP, choroid plexus papilloma; Cr, creatine; CRLB, Cramér-Rao lower bound; DNET, dysembryoplastic neuroepithelial tumour; FWHM, full-width at half maximum; GBM, glioblastoma; Gly, glycine; hTau, hypotaurine; HRMAS, high-resolution magic angle spinning; mI, myo-inositol; PA, pilocytic astrocytoma; PCh, phosphocholine; PRESS, point-resolved spectroscopy; SD, standard deviation; sI, scyllo-inositol; SNR, signal-to-noise ratio; T, Tesla; Tau, taurine; TMSP, trimethylsilicyl proprionate d4; WHO, World Health Organization.*

inaccurate basis sets lead to inaccurate metabolite profiles (6,9). This may occur due to distortions of the estimated baseline in an attempt to account for unmodelled peaks and/or false assignment of overlapping signals arising from metabolites not present in the basis set. A systematic study of the effects of different basis set compositions on metabolite quantitation based on MRS of normal brain has suggested that the inclusion of additional metabolites beyond those that contribute the major signals to the spectra can lead to stable and robust fits, even if they are present in sub-millimolar concentrations (10). One approach to optimising basis sets for *in-vivo* MRS is to use information from biological and *ex-vivo* studies in combination with analysis of the LCModel™ fit residues to expand the basis set in a hypothesis driven manner (6). This approach has been used here to investigate the *in-vivo* detection of glycine (Gly) in $^1$H MRS performed on a clinical MRI scanner with a field-strength of 1.5 Tesla.

Glycine (Gly), an inhibitory neurotransmitter, is the smallest amino acid with a concentration estimated to be approximately 1 mM in the normal adult brain (11) and the developing brain (12), although the concentration has been shown to vary significantly across certain brain regions in the rat brain (13). Gly has recently been identified as a potential biomarker in brain tumours (14). Previous reports from *in-vitro* studies have shown that Gly increases with WHO grade and is high in medulloblastomas and glioblastomas (15–20). Similar findings have been observed *in vivo* in a rat glioma model (21). High-resolution magic angle spinning (HRMAS) spectra from biopsy samples of paediatric high-grade brain tumours have been shown to contain high Gly signals (22). Accurate discrimination of Gly and mI *in vivo* may provide a biomarker for improved diagnosis and prognosis of brain tumours (23). Gly is not usually included separately in linear combination models of MR spectra because the singlet peak of Gly at approximately 3.55 ppm strongly overlaps with the multiplet peak of myo-inositol (mI) around 3.6 ppm. Most MRS studies of brain tumours have used a single echo time (TE), either short (~30 ms) or long (~135 ms). The discrimination of Gly and mI signals is more likely at long TE since the mI signal is attenuated relative to Gly due to strong J-coupling effects. However, this comes at the expense of additional information available at short TE, particularly from macromolecules and lipids, that could be useful for classification. This may be problematic where acquisition at both short and long TE is not possible due to time constraints.

The aim of this study was to investigate Gly quantitation in childhood brain tumours using single-voxel MRS at short and long TE analysed by LCModel™. High-resolution magic angle spinning (HRMAS) NMR of matched tumour biopsy samples has been used as a comparison, since the discrimination of Gly and mI is relatively simple at high field-strengths.

## PATIENTS AND METHODS

Single-voxel $^1$H MRS was performed as part of a clinical MR protocol designed for scanning children with suspected brain tumours on a Siemens Symphony Magnetom 1.5 T scanner. Ethical approval was given for the study by the Local Research Ethics Committee and parental consent was obtained. MRS was acquired using the PRESS sequence with a TR of 1500 ms and a TE of 30 ms ('short') or 135 ms ('long'). Cubic voxels were placed to fit within the contrast enhancing or most solid part of the tumour visualised on the standard MR images with side length of either 1.5 cm or 2.0 cm according to the size of the tumour target. For the smaller voxels 256 repetitions were used for signal averaging while for the larger voxels 128 repetitions were used. In the cases where large voxels were used, both short and long TE MRS was performed where time constraints allowed. Additional spectra were acquired without water suppression, while keeping all other parameters constant, providing a reference for metabolite concentrations. For patients undergoing surgery subsequent to the MRI study, biopsy samples were made available for *ex-vivo* investigation where sufficient tumour material was available. HRMAS was performed on biopsy samples from 16 patients using a pulse-acquire sequence on a Varian 600 MHz spectrometer with a gHX nanoprobe spun at 2.5 kHz and a sample temperature of 6.7°C [see ref (22) for further details].

Two cohorts were retrospectively selected from the group of children with suspected brain tumours studied prior to treatment between March 2003 and October 2008. The first cohort consisted of those cases for which short-TE MRS was acquired *in vivo* and HRMAS was performed on a corresponding tumour sample. The second group consisted of the patients where both short-TE and long-TE spectra were acquired *in vivo*. Table 1 shows the number of cases meeting these criteria and the mix of tumour diagnoses represented in each group. The groups were mutually exclusive, with the exception of one patient with a pilocytic astrocytoma who had all three types, providing a combined group of 47 cases for which short-TE MRS was available with either long-TE MRS or *ex-vivo* HRMAS for comparison. The diagnosis was confirmed by histopathology for 36 patients with 15 medulloblastomas (MB), 12 pilocytic astrocytomas (PA), two glioblastomas (GBM), three ependymoma and one each of germinoma, choroid plexus papilloma (CPP), ganglioglioma and diffuse astrocytoma. Of these, 18 were confirmed to be high grade (World Health Organization (WHO) grade III and IV) tumours (including one anaplastic ependymoma) and 17 were identified as low grade (WHO grade I and II) tumours. The other 11 patients were diagnosed using clinical and radiological criteria as four diffuse pontine gliomas (DPG), two dysembryoplastic neuroepithelial tumours (DNET), and 5 non-tumour space occupying lesions.

*In-vivo* spectra were processed by LCModel™ (version 6.2–0) using two basis sets, one including Gly and one excluding Gly. Each metabolite signal in the basis set was simulated based on the appropriate PRESS sequence parameters using the density matrix formalism and published data for metabolite chemical shifts and coupling constants (24,25). The other metabolites included in the basis set were: alanine, aspartate, creatine (Cr), $\gamma$-aminobutyric acid, glucose, glutamine, glutamate, myo-inositol (mI), lactate, N-acetyl-aspartate, N-acetylaspartylglutamate, scyllo-inositol (sI), taurine (Tau), glycero-phosphocholine, phosphocholine (PCh) and guanidinoacetate. Nine simulated lipid and macromolecular components provided with this version of LCModel™ were also included at around 0.9 ppm (× 2), 1.2 ppm, 1.3 ppm (× 2), 1.4 ppm, 1.7 ppm and 2.0 ppm (× 2). In addition, a correction term for the CH2 peak of Cr at 3.9 ppm was included to account for saturation caused by the water suppression pulses.

Concentrations were determined relative to the corresponding water spectrum. In the absence of well-defined values for the water content and $T_2$ of childhood brain tumours, a constant water content and $T_2$ equivalent to that of grey matter was assumed (concentration: 43.3 M, $T_2$: 80 ms (26)). Quality control (QC) of the spectra was carried out such that they were excluded if the voxel was misplaced, the signal-to-noise ratio $< 4$, or the

**Table 1.** Recruitment of patients to the study according to tumour type and grade and the availability of short-TE and long-TE *in-vivo* MRS and matched HRMAS data

| Grade | Type | Short-TE MRS + HRMAS | Short + Long-TE MRS | Total |
|---|---|---|---|---|
| High Grade | Medulloblastoma | 8 | 7 | 15 |
| | Glioblastoma | | 2 | 2 |
| | Anaplastic Ependymoma | 1 | | 1 |
| Low Grade | Pilocytic Astrocytoma | 5 | 8 | 12 |
| | Ependymoma | 1 | 1 | 2 |
| | Diffuse Astrocytoma | | 1 | 1 |
| | Ganglioglioma | | 1 | 1 |
| | Choroid Plexus Papilloma | | 1 | 1 |
| Ungraded | Germinoma | | 1 | 1 |
| Unbiopsied | Diffuse Pontine Glioma | | 4 | 4 |
| | DNET | | 2 | 2 |
| Non-tumour space occupying lesions | | | 5 | 5 |
| Total | | 15 | 33 | 47 |

water linewidth (full-width-at-half maximum, FWHM) > 10 Hz. To compare the quality of fits obtained using the simulated basis set containing Gly with those obtained using a basis set excluding Gly, the root-mean-square (RMS) of the fit residues (signal – fit) between 3.3 ppm and 3.7 ppm was computed. Paired Student's *t*-tests were used to test the null hypothesis that there is no difference in the RMS of the fit residues obtained with and without Gly in the basis set for both short-TE and long-TE MRS. Furthermore, the possible difference in the RMS of the fit residues in the 3.3 to 3.7 ppm range with and without Gly (normalised to the RMS of the fit residues between 0.5 ppm and 4 ppm) was compared between high grade and low grade tumours using unpaired two-tailed Student's *t*-tests assuming unequal variances. The Cramér-Rao Lower Bounds (CRLB) estimates reported by LCModel™ were used to assess the reliability of the Gly fits.

The hypothesis that Gly concentrations estimated by LCModel™ are higher in high grade tumours than low grade tumours was tested using two-tailed Student's *t*-tests assuming unequal variances for both the short-TE and long-TE spectra. In the group for which both short-TE and long-TE spectra were obtained, agreement between the Gly concentrations estimated at each TE was investigated by determining the Pearson's correlation coefficient. For the group with HRMAS data, spectra were fitted using the TARQUIN algorithm (27) and the Gly and mI concentrations normalised by the sum of all metabolite concentrations were compared between low grade and high grade tumours and correlated with the *in-vivo* results.

## RESULTS

After applying the QC criteria, five cases were excluded from the group with both short-TE and long-TE data, representing two pilocytic astrocytomas, one germinoma and two non-tumour lesions. In the remaining spectra, the LCModel™ fits were found to be significantly improved by the inclusion of Gly in the basis set for both long-TE ($p < 0.05$) and short-TE spectra ($p < 0.05$), using paired *t*-tests of the RMS of the residues between 3.3 ppm and 3.7 ppm. The magnitude of the improvement obtained using a basis set including Gly was greater for the long-TE spectra, with a mean fractional decrease of 8% in the RMS of the residues compared with 2% for the short-TE spectra. Table 2 demonstrates that this improvement was confined almost entirely to the spectra from high grade tumours with a mean decrease in RMS of the residues in this spectral range of 22% at long TE and 5% at short TE.

Figure 1 illustrates the improvement in the spectral fits resulting from the inclusion of Gly in the basis set for long TE and short TE spectra from a representative high grade tumour (medulloblastoma, grade 4). The improvement in the fit with Gly can be clearly seen for the long-TE spectrum, with a markedly reduced residue (data – fit) in the range 3.3–3.7 ppm and a flatter baseline across a broader region of the spectrum. A similar but more subtle improvement can also be appreciated in the short-TE fit.

Figure 2 shows a scatter plot of the Gly concentrations measured at long TE and short TE revealing a highly significant correlation (Pearson's correlation coefficient, $R = 0.91$, $p < 0.001$). The line of best fit suggests less than 20% discrepancy between the values estimated at short TE and long TE, with a tendency for higher estimates at long-TE. However, at lower concentrations the short-TE spectra sometimes give a higher estimate of Gly concentration. The error bars depicting the CRLB for each fit show that for higher concentrations, the uncertainty of the quantitation is less than 20% for both long and short TE. As indicated in the plot, the high grade tumours have a significantly higher Gly

**Table 2.** Mean fractional fit improvement after including glycine in the basis set at long TE (135 ms) and short TE (30 ms) for high grade *vs* low grade tumours

| | Fractional decrease in RMS of residues between 3.3–3.7 ppm | | | | |
|---|---|---|---|---|---|
| | High Grade (HG) | | Low Grade (LG) | | HG vs LG |
| | Mean | SD | Mean | SD | P |
| Long TE | +0.22 | 0.17 | +0.01 | 0.03 | <0.001 |
| Short TE | +0.05 | 0.06 | −0.01 | 0.02 | <0.001 |

NMR IN BIOMEDICINE

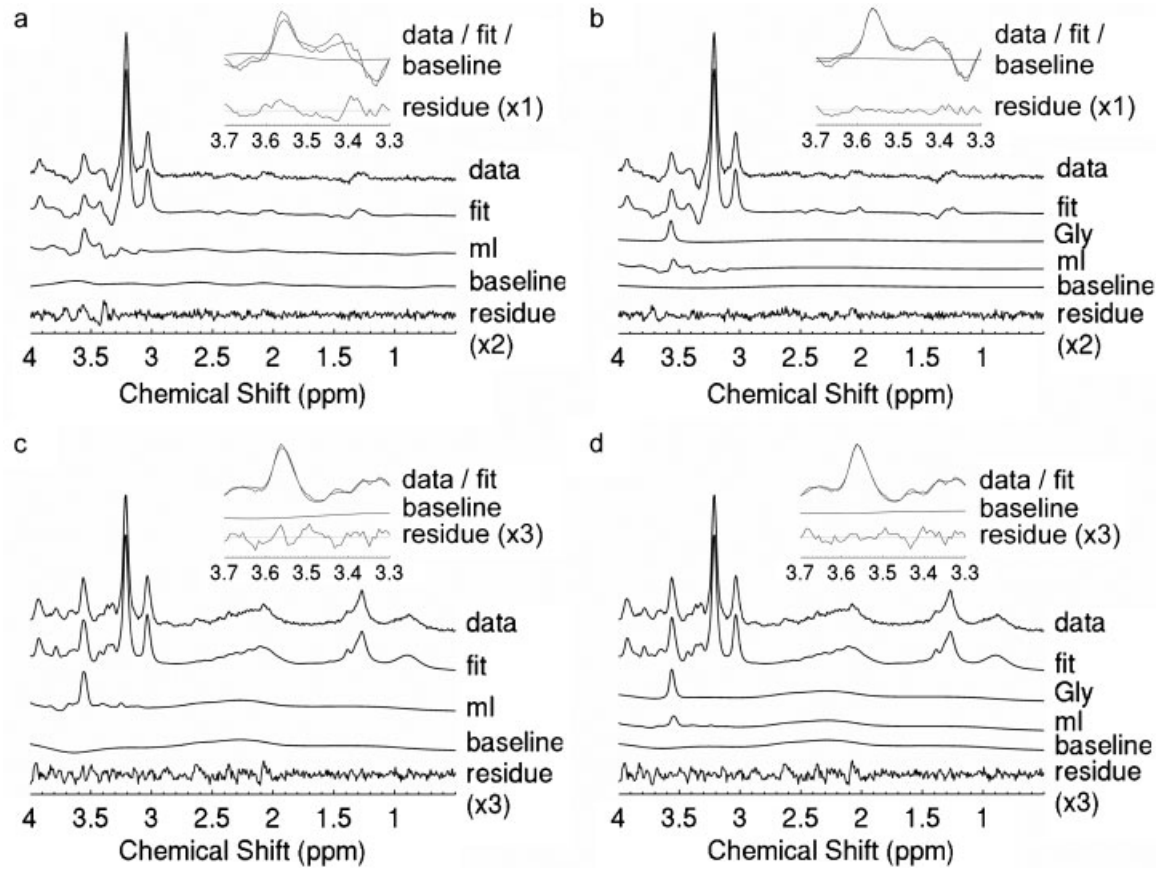


**Figure 1.** Example spectra from a medulloblastoma with LCModel$^{TM}$ fits at long TE (a) without glycine (Gly) in the basis set and (b) with Gly included in the basis set and at short TE (c) without Gly in the basis set and (d) with Gly included in the basis set. The complete fits, individual metabolite fits for myo-inositol (ml) and Gly, estimated baseline and fit residues are shown offset beneath the spectra. Inset in each panel is an expanded view of the 3.3–3.7 ppm region containing the overlapping Gly and ml signals showing a collapsed view of the data, fit and baseline with the residue offset. The residues have been scaled by the factor indicated to allow improvements in the residues around 3.5 ppm to be seen more clearly.

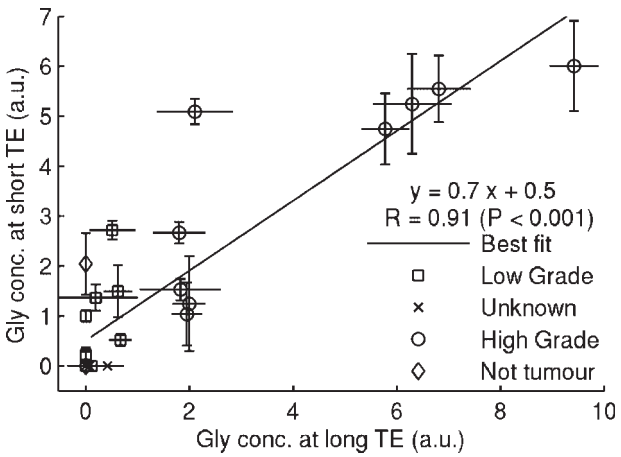


**Figure 2.** Correlation of glycine concentrations obtained from LCModel$^{TM}$ analysis of corresponding MR spectra using long TE (135 ms) and short TE (30 ms) with high grade (circles), low grade (squares), unknown grade (crosses) and non-tumour (diamonds) cases indicated. Error bars represent uncertainties (CRLB) reported by LCModel$^{TM}$. The line of best fit (solid) results from a robust least squares fitting algorithm (Pearson's correlation coefficient, $R = 0.91$; $p < 0.001$).

concentration than the low grade tumours. There is a consistent separation between the high grade and low grade tumours based on the Gly concentration estimated from the long-TE MRS.

Table 3 records the mean Gly concentrations measured for low and high grade tumours at short and long TE. The difference in Gly concentration between high grade and low grade tumours is highly significant when estimated from both the short-TE spectra and long-TE spectra. For the high-grade tumours with greater estimated Gly concentration, the accuracy is equivalent for short-TE and long-TE fits (mean CRLB 19%). The two GBMs have a lower estimated Gly concentration than the rest of the high-grade group consisting of medulloblastomas. The estimated Gly concentration for these cases is 1.4 mM and 1.2 mM with CRLB of 71% and 66% respectively for the short-TE fits and 2.4 mM and 2.3 mM with CRLB of 16% and 15% respectively for the long-TE fits, showing an improved accuracy at long-TE in these cases. The anaplastic ependymoma (grade III) that did not have long-TE MRS had a high Gly concentration from short-TE MRS (4.1 mM, CRLB 26%), whereas the two low-grade ependymomas did not have a measurable Gly concentration *in vivo* at short-TE or long-TE. For the low-grade tumours the majority of the glycine values had CRLB > 50% at both short-TE and long-TE implying that the metabolite was below the level at which it could be reliably detected in these tumours. Five low-grade tumours (three PA, one CPP, one ganglioglioma) had Gly concentrations from short-TE MRS estimated with CRLB < 50%. Of the four of these that also



  

**Table 3.** Comparison of mean glycine concentrations and mean Cramer Rao Lower Bounds (CRLB) from LCModel™ fits to short and long TE spectra for high grade and low grade, with *p* values from Student's t-tests assuming unequal variances

| | Glycine concentration for high grade vs low grade tumours at short and long TE (mM) | | | |
|---|---|---|---|---|
| | Short TE | | Long TE | |
| | Mean conc. | SD | Mean conc. | SD |
| High Grade | 3.9* | 2.0 | 5.1** | 3.5 |
| Low Grade | 0.4† | 0.6 | 0.2†† | 0.3 |
| *p*-value | < 1e–6 | | 0.003 | |

*$n = 18$; †$n = 15$; **$n = 9$; ††$n = 10$.

had long-TE MRS (two PA, one CPP, one ganglioglioma), Gly was detected with CRLB < 50% in two (one PA, one CPP), but not detected in the other two. Of these low-grade cases where Gly was reliably detected it was at a level below that of all the high-grade tumours.

Figure 3 shows representative HRMAS spectra from a high grade and low grade tumour focussing on the 3.3–3.7 ppm region. In the spectrum from the high grade tumour, there is a prominent singlet peak at 3.55 ppm attributed to glycine that is clearly distinguished from the multiplet peak of myo-inositol. This is not the case in the spectrum from the low-grade tumour, although small amounts of Gly could be quantified in some of the low-grade tumours. Figure 4 shows that the normalised Gly concentrations measured by the TARQUIN analysis of the HRMAS spectra correlate significantly with the corresponding normalised values measured by LCModel™ from the short-TE *in-vivo* MRS (Pearson's correlation coefficient: $R = 0.57$, $p < 0.05$). Two-tailed Student's t-tests showed a significantly higher normalised Gly concentration for the high grade tumours (medulloblastomas) compared with the low grade tumours for both the HRMAS ($p < 0.05$) and *in-vivo* ($p < 0.0001$) data. In addition, the normalised mI concentrations were significantly correlated between the short-TE in-vivo MRS and the corresponding HRMAS NMR spectra ($R = 0.76$, $p < 0.01$). However, no significant differences in normalised mI were found between the high grade and low grade tumours.

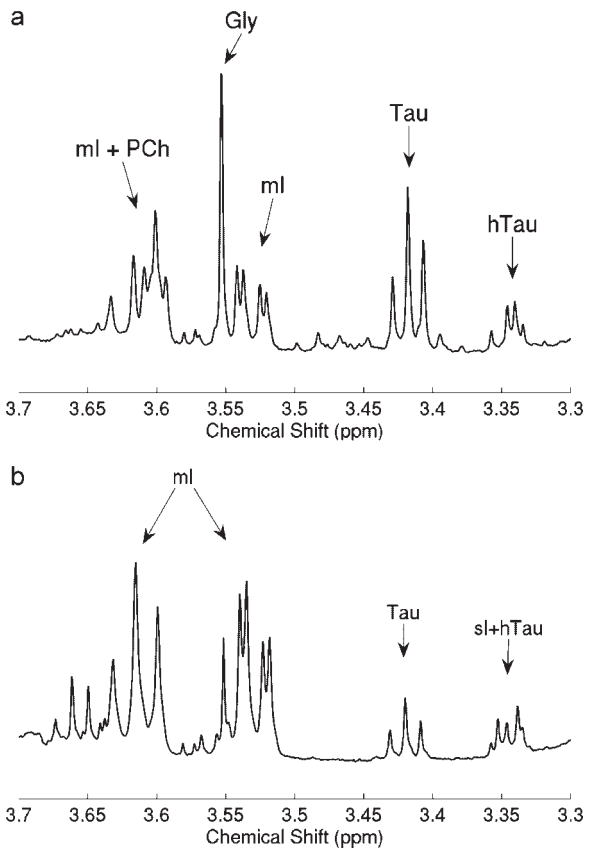


**Figure 3.** High-resolution magic angle spinning (HRMAS) NMR spectra showing the spectral region from 3.3–3.7 ppm for typical (a) medulloblastoma (high grade) and (b) pilocytic astrocytoma (low grade) biopsy samples, showing the presence of glycine in the high grade spectrum. Gly, glycine; hTau, hypotaurine; mI, myo-Inositol; sI, scyllo-inositol; Tau, taurine.

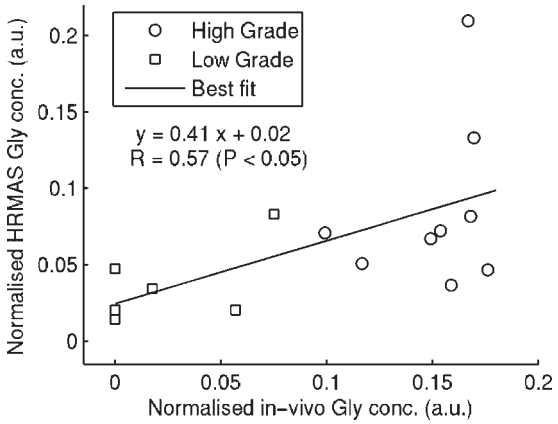


**Figure 4.** Correlation of normalised Gly concentration measured from LCModel analysis of short-TE in-vivo MRS and TARQUIN analysis of corresponding HRMAS NMR spectra of matched surgical samples. High grade (circles) and low grade tumours (squares) are indicated, along with the best linear fit (Pearson's correlation coefficient, $R = 0.57$, $p < 0.05$).

The PA with Gly estimated with CRLB < 50% in both short-TE (0.6 mM, CRLB 23%) and long-TE (0.8 mM, CRLB 33%) *in-vivo* MRS also underwent HRMAS, which showed the highest normalised Gly concentration of the eight low-grade tumours. In addition, the HRMAS results showed a normalised Gly concentration for the high-grade ependymoma 2.6 times as high as for the low-grade ependymoma.

## DISCUSSION

In this study, MR spectra of childhood brain tumours *in vivo* and *ex vivo* (using HRMAS) have been analysed to assess the capability of single voxel MRS at 1.5 Tesla to non-invasively detect and measure glycine levels. The results demonstrate that LCModel™ fits to *in-vivo* spectra acquired at both long TE and short TE are significantly improved by including glycine in the basis set. As expected due to the attenuation and modulation of the mI signal at long TE caused by the strong J-coupling in this molecule, the magnitude of the fit improvement is much greater for the long TE spectra than the short TE spectra. Nevertheless, the highly

NMR IN BIOMEDICINE

significant improvement resulting from including glycine in the fits at short TE together with the strong correlation of the glycine concentrations measured at the different TE and the relatively low CRLB in most cases, suggest that glycine can be reliably detected *in vivo* by MRS at a field-strength of 1.5 Tesla using both long and short TE. Further evidence for this is provided by the significant correlations in the normalised Gly and mI concentrations between short-TE *in-vivo* MRS and HRMAS of corresponding biopsy samples.

Analysis of the CRLB estimates of the LCModel$^{TM}$ quantitation as a function of the Gly concentration (not shown) indicates that for good quality spectra the minimum concentration of Gly that can be reliably detected with a CRLB $< 50\%$ is approximately $0.9 \pm 0.6$ mM. This limit will depend on the quality of the individual spectrum, the relative concentrations of Gly and mI in the tumour, and the presence of other overlapping signals. The trend towards higher estimates of Gly concentration in the long-TE relative to the short-TE MRS at high Gly levels may be the result of unaccounted-for differences in $T_2$ between water and Gly in these tumours, or under estimation of the short-TE Gly concentration due to the stronger overlap with mI. There is some evidence to suggest that low Gly concentrations can be estimated by short-TE MRS in some low-grade tumours. In these cases, where the SNR is inherently low due to lower cell density the further reduction in SNR at long-TE leads to less reliable Gly detection and lower estimates of Gly concentration (Fig. 2). Alternatively, it is possible that Gly concentrations may be over estimated at short-TE in some low grade tumours for which the spectral quality is less good, particularly with low SNR. However, the low-grade tumour with the highest normalised Gly concentration measured by HRMAS also gave the most consistent estimate of Gly concentration and CRLB between the short-TE and long-TE *in-vivo* MRS among the low-grade tumours.

Good evidence has been shown for the detection of a high concentration of glycine in high-grade paediatric brain tumours using short-TE and long-TE *in-vivo* MRS at 1.5 T, which is in agreement with *in-vitro*, *ex-vivo* and animal studies that implicate Gly as a potential biomarker for malignancy in brain tumours (14–21). This finding held true for the small number of high-grade glial tumours in this study, suggesting that there is the potential to strengthen the biomarker profile of high-grade tumours by including Gly in spectral fitting models and hence improve the performance of classifiers based on metabolite profiles for high-grade versus low-grade brain tumours (28). It should be noted that the absolute Gly concentrations estimated in this study did not take account of water content or $T_2$ variations between the high-grade and low-grade tumours that may exist due to variations in cellular density. The largest effect is likely to arise from tissue water content variations. Water content is likely to be higher in brain tumours than the grey matter value used here of approximately 80%, with higher values in the pilocytic astrocytomas (low grade) than high-grade tumours. Whilst this may lead to an underestimate of the Gly concentration in this study and a bias towards lower concentrations in the low-grade tumours, these effects are likely to be less than 10–20%.

The current dataset is dominated by medulloblastomas and pilocytic astrocytomas and greater numbers in the other tumour groups are required to confirm the relationship of Gly concentration with grade. Perhaps more importantly from a clinical perpective, follow-up data is required on the patients to evaluate Gly as a prognostic marker independent of grade in childhood brain tumours. Further study is also warranted to investigate the potential impact of Gly detection on the discrimination and prognosis of brain tumours in adults using MRS (14).

The biological significance of the elevated Gly levels seen in malignant tumours is unclear. Recently, the role of Gly as an inhibitory neurotransmitter and its involvement in brain metabolism has led to several studies investigating the non-invasive measurement of Gly with MRS carried out at high magnetic fields (29–32). However, little has been documented of the ability to detect and quantify Gly *in vivo* with MRS at 1.5 T. To our knowledge, this is the first study to provide evidence to support the robust quantitation of Gly at 1.5 T. Some studies have suggested that detection of Gly is possible at this field strength in different pathologies (33–37), indicating that this approach may have applications beyond brain tumour characterisation. This study has utilised existing MRS data acquired with standard protocols, but if Gly quantitation is taken to be the primary goal, optimisation of the PRESS sequence parameters can be implemented to minimise the overlap of Gly and mI at 3.55 ppm and thereby enhance the Gly quantitation (32). This may be necessary to allow robust quantitation of Gly levels in cases where SNR is limited, in tumours with high levels of mI and in adult glioblastomas and metastases where metabolite signals are notoriously difficult to assess due to the high levels of lipids present.

Observations of paediatric brain tumour spectra and fit residues in our study indicate that some signals are still unaccounted for in the fits, indicating that further optimisation of the LCModel$^{TM}$ basis set for the study of brain tumour metabolism is possible. Other studies have shown that the addition of metabolites such as glutathione to an experimental LCModel$^{TM}$ basis set improves the characterisation of brain tumours in adults (6). This study has shown that using simulation based on known parameters is a feasible and convenient method for expanding spectral fitting basis sets. Further analysis leading to increasingly detailed assignments of signals in the HRMAS spectra of biopsy samples and re-simulations of such signals at 1.5 T for inclusion in the basis set for LCModel$^{TM}$ (or an alternative LC spectral fitting tool), followed by rigorous assessment of the improvement in the fits of the *in-vivo* spectra may allow the detection of so far unaccounted for metabolites and thus improve our understanding of the underlying tumour metabolism. This approach may be used in conjunction with an alternative method that uses independent components analysis for distinguishing individual metabolite signals within spectra, potentially leading to the identification of unexpected metabolite signals (38).

## CONCLUSIONS

LCModel$^{TM}$ analysis can be used to reliably detect glycine in paediatric brain tumours using both short-TE and long-TE MRS at a field strength of 1.5 Tesla. This has been shown by the significant reduction in the LCModel$^{TM}$ fit residues resulting from the inclusion of Gly in the basis set, the significant correlation of the Gly concentrations estimated from the short-TE and long-TE spectra, and the significant correlation of the normalised Gly and mI concentrations between the short-TE *in-vivo* MRS and the *ex-vivo* HRMAS analysis. Furthermore, the Gly concentration estimated by LCModel$^{TM}$ was significantly higher in the high



  

grade brain tumours compared with the low grade brain tumours for both short-TE and long-TE MRS, consistent with the HRMAS results and with previous *in-vitro* studies. This study highlights the validity and importance of including Gly in the LCModel™ basis set for the study of brain tumours and the potential contribution of Gly quantitation to the biomarker profile of malignancy.

## Acknowledgements

The authors would like to acknowledge the important role played by the staff of the Radiology Department at Birmingham Children's Hospital and in particular Shaheen Lateef for her efforts in helping to acquire the *in-vivo* MRS data and Rachel Grazier for help in organising the data collection. This work was part funded by the European Union Framework 6 project eTumour, the UK Medical Research Council, the Department of Health, Birmingham Children's Hospital Research Foundation, the Joe Foote and Alistair Wainwright Foundations and Poppy Fields Charity. ACP was funded by a Department of Health National Clinician Scientist Award.

## REFERENCES

1. Preul MC, Caramanos Z, Collins DL, Villemure JG, Leblanc R, Olivier A, Pokprupa R, Arnold DL. Accurate, noninvasive diagnosis of human brain tumors by using proton magnetic resonance spectroscopy. Nat Med. 1996; 2: 323–325.
2. Tate AR, Majos C, Moreno A, Howe FA, Griffiths JR, Arus C. Automated classification of short echo time in *in vivo* 1H brain tumor spectra: a multicenter study. Magn Reson Med. 2003; 49: 29–36.
3. García-Gómez JM, Luts J, Julià-Sapé M, Krooshof P, Tortajada S, Robledo JV, Melssen W, Fuster-García E, Olier I, Postma G, Monleón D, Moreno-Torres A, Pujol J, Candiota AP, Martínez-Bisbal MC, Suykens J, Buydens L, Celda B, Van Huffel S, Arús C, Robles M. Multiproject-multicenter evaluation of automatic brain tumor classification by magnetic resonance spectroscopy. Magn Reson Mater Phy. 2009; 22: 5–18.
4. Opstad KS, Ladroue C, Bell BA, Griffiths JR, Howe FA. Linear discriminant analysis of brain tumour (1)H MR spectra: a comparison of classification using whole spectra versus metabolite quantification. NMR Biomed. 2007; 20: 763–770.
5. Davies NP, Wilson M, Harris LM, Natarajan K, Lateef S, MacPherson L, Sgouros S, Grundy RG, Arvanitis TN, Peet AC. Identification and characterisation of childhood cerebellar tumours by *in vivo* proton MRS. NMR Biomed. 2008; 21: 908–918.
6. Opstad KS, Provencher SW, Bell BA, Griffiths JR, Howe FA. Detection of Elevated Glutathione in Meningiomas by Quantitative *In vivo* 1H MRS. Magn Reson Med. 2003; 49: 632–637.
7. Opstad KS, Bell BA, Griffiths JR, Howe FA. Taurine: a potential marker of apoptosis in gliomas. Br J Cancer. 2009; 100: 789–794.
8. Provencher SW. Estimation of metabolite concentrations from localized *in vivo* proton NMR spectra. Magn Reson Med. 1993; 30: 672–679.
9. Hofman L, Boesch C, Kreis R. Influence of the composition of the basis set in linear combination model fitting of $^{1}$H-MR spectra of human brain. *Proceedings of the 10th Annual Meeting ISMRM*, Honolulu, USA, 2002; 527.
10. Hofman L, Slotboom J, Jung B, Maloca P, Boesch C, Kreis R. Quantitative $^{1}$H-magnetic resonance spectroscopy of human brain: influence of composition and parameterization of the basis set in linear combination model-fitting. Magn Reson Med. 2002; 48: 440–453.
11. Kinoshita Y, Kajiwara H, Yokota A, Koga Y. Proton magnetic resonance spectroscopy of brain tumors: an in vitro study. Neurosurgery. 1994; 35: 606–614.
12. Kreis R, Hofmann L, Kuhlmann B, Boesch C, Bossi E, Hüppi PS. Brain metabolite composition during early human brain development as measured by quantitative *in vivo* 1H magnetic resonance spectroscopy. Magn Reson Med. 2002; 48: 949–958.
13. Xin L, Gambarota G, das Neves Duarte J, Mlynarik V, Gruetter R. Glycine tissue level in medulla oblongata measured *in vivo* with $^{1}$H MRS at 9.4 T in rat brain. *Proceedings of the 17th Annual Meeting ISMRM*, Honolulu, USA, 2009; 3291.
14. Righi V, Mintzopoulos D, Andronesi OC, Black PM, Tzika AA. Glycine as a biomarker in brain tumors. *Proceedings of the 17th Annual Meeting ISMRM*, Honolulu, USA, 2009; 198.
15. Carpinelli G, Carapella CM, Palombi L, Raus L, Caroli F, Podo F. Differentiation of glioblastoma multiforme from astrocytomas by in vitro 1H MRS analysis of human brain tumors. Anticancer Res. 1996; 16: 1559–1563.
16. Kinoshita Y, Yokota A. Absolute concentrations of metabolites in human brain tumors using in vitro proton magnetic resonance spectroscopy. NMR Biomed. 1997; 10: 2–12.
17. Carapella CM, Carpinelli G, Knijn A, Raus L, Caroli F, Podo F. Potential role of in vitro $^{1}$H magnetic resonance spectroscopy in the definition of malignancy grading of human neuroepithelial brain tumours. Acta Neurochir Suppl. 1997; 68: 127–132.
18. Roda JM, Pascual JM, Carceller F, González-Llanos F, Pérez-Higueras A, Solivera J, Barrios L, Cerdán S. Nonhistological Diagnosis of Human Cerebral Tumors by $^{1}$H Magnetic Resonance Spectroscopy and Amino Acid Analysis. Clin Cancer Res. 2000; 6: 3983–3993.
19. Lehnhardt FG, Röhn G, Ernestus RI, Grüne M, Hoehn M. 1H- and (31)P-MR spectroscopy of primary and recurrent human brain tumors in vitro: malignancy-characteristic profiles of water soluble and lipophilic spectral components. NMR Biomed. 2001; 14: 307–317.
20. Lehnhardt FG, Bock C, Röhn G, Ernestus RI, Hoehn M. Metabolic differences between primary and recurrent human brain tumors: a $^{1}$H NMR spectroscopic investigation. NMR Biomed. 2005; 18: 371–382.
21. Gyngell ML, Hoehn-Berlage M, Kloiber O, Michaelis T, Ernestus RI, Hörstermann D, Frahm J. Localized proton NMR spectroscopy of experimental gliomas in rat brain *in vivo*. NMR Biomed. 1992; 5: 335–340.
22. Wilson M, Davies NP, Brundler MA, McConville C, Grundy RG, Peet AC. High resolution magic angle spinning 1H NMR of childhood brain and nervous system tumours. Mol Cancer. 2009; 8: 6.
23. Mader I, Roser W, Hagberg G, Schneider M, Sauter R, Seelig J, Radue EW, Steinbrich W. Proton chemical shift imaging, metabolic maps, and single voxel spectroscopy of glial brain tumors. Magn Reson Mater Phy. 1996; 4: 139–150.
24. Wilson M, Davies NP, Sun Y, Natarajan K, Arvanitis TN, Peet AC. A comparison between simulated and experimental basis sets for the analysis of short-echo in-vivo MRS data at 1.5 T. *Proceedings of the 17th Annual Meeting ISMRM*, Honolulu, USA, 2009; 4337.
25. Govindaraju V, Young K, Maudsley AA. Proton NMR chemical shifts and coupling constants for brain metabolites. NMR Biomed. 2000; 13: 129–1153.
26. Tong Z, Yamaki T, Harada K, Houkin K. In vivo quantification of the metabolites in normal brain and brain tumors by proton MR spectroscopy using water as an internal standard. Magn Reson Imaging. 2004; 22: 1017–1024.
27. Reynolds G, Wilson M, Peet A, Arvanitis TN. An algorithm for the automated quantitation of metabolites in in vitro NMR signals. Magn Reson Med. 2006; 56: 1211–1219.
28. Davies NP, Wilson M, Harris LM, MacPherson L, Brundler MA, Arvanitis TN, Grundy RG, Peet AC. Pattern recognition of single voxel 1H MRS metabolite profiles for classification and characterisation of childhood brain tumours according to type and grade. Magn Reson Mater Phy. 2008; 21(S1): 18.
29. Prescot AP, de B Frederick B, Wang L, Brown J, Jensen JE, Kaufman MJ, Renshaw PF. In vivo detection of brain glycine with echo-time-averaged (1)H magnetic resonance spectroscopy at 4.0 T. Magn Reson Med. 2006; 55: 681–686.
30. Choi C, Bhardwaj PP, Seres P, Kalra S, Tibbo PG, Coupland NJ. Measurement of glycine in human brain by triple refocusing 1H-MRS *in vivo* at 3.0 T. Magn Reson Med. 2008; 59: 59–64.
31. Gambarota G, Mekle R, Xin L, Hergt M, van der Zwaag W, Krueger G, Gruetter R. In vivo measurement of glycine with short echo-time (1)H MRS in human brain at 7 T. Magn Reson Mater Phy. 2009; 22: 1–4.
32. Choi C, Dimitrov L, Douglas D, Hawesa H. Measurement of glycine in human brain by PRESS at 7.0 Tesla *in vivo*. *Proceedings of the 17th Annual Meeting ISMRM*, Honolulu, USA, 2009; 2397.

33. Heindel W, Kugel H, Roth B. Noninvasive detection of increased glycine content by proton MR spectroscopy in the brains of two infants with nonketotic hyperglycinemia. Am J Neuroradiol. 1993; 14: 629–6635.
34. Huisman TA, Thiel T, Steinmann B, Zeilinger G, Martin E. Proton magnetic resonance spectroscopy of the brain of a neonate with nonketotic hyperglycinemia: in vivo-in vitro (ex vivo) correlation. Eur Radiol. 2002; 12: 858–861.
35. Yeh IB, Xu M, Ng WH, Ye J, Yang D, Lim CC. Central neurocytoma: typical magnetic resonance spectroscopy findings and atypical ventricular dissemination. Magn Reson Imaging. 2008; 26: 59–64.
36. Malik GK, Pandey M, Kumar R, Chawla S, Rathi B, Gupta RK. MR imaging and *in vivo* proton spectroscopy of the brain in neonates with hypoxic ischemic encephalopathy. Eur J Radiol. 2002; 43: 6–13.
37. Sener RN. The glycine peak in brain diseases. Comput Med Imag Grap. 2003; 27: 297–305.
38. Hao J, Zou X, Wilson MP, Davies NP, Sun Y, Peet AC, Arvanitis TN. A comparative study of feature extraction and blind source separation of independent component analysis (ICA) on childhood brain tumour 1H magnetic resonance spectra. NMR Biomed. 2009; Published Online: 8 May 2009.